Staurosporine restores GTPγS induced block of rapid endocytosis in chromaffin cells

Andreas Wolfram Henkel*, Tobias Kristian Vogt, Maria Kerstin Henkel

Department of Psychiatry (Molecular Neurobiology), University of Erlangen – Nuremberg, Schwabachanlage 6, 91054 Erlangen, Germany

Received 7 April 2004; revised 7 June 2004; accepted 21 June 2004

Available online 6 July 2004

Edited by Lukas Huber

Abstract Fast capacitance measurements demonstrated that chromaffin cells retrieve membrane by several kinetically different pathways. Here, we show that rapid endocytosis is blocked and slow endocytosis reduced by intracellular application of GTPγS, an activator of G-proteins, but not by the competitive blocker GDPβS. The inhibition of rapid endocytosis by GTPγS can be restored with GDPβS or staurosporine completely. But only staurosporine partially abolishes the reduction of slow endocytosis by GTPγS. Besides triggering exocytosis, GTPγS elicits large exo- and endocytotic vesicles that contributed significantly to the total membrane traffic, indicating a third pathway of membrane shuttle.

Keywords: Capacitance measurement; Bovine chromaffin cell; Endocytosis; GTP-gamma-S; Staurosporine

1. Introduction

Extent and speed of endocytosis after stimulated exocytosis in chromaffin cells varies considerably, depending on the strength of the stimulus, the internal calcium concentration and the physiological status of the cell [1,2]. The molecular endocytotic machinery enfolds kinases and phosphatases to modulate the endocytotic protein complex, consisting of clathrin, adaptor proteins, dynamin, amphyphisin and many other regulatory proteins [3,4]. There is certainly more than one mechanism for membrane retrieval besides the classical pathway that involves clathrin-coated vesicles.

It has been shown that endocytosis takes place with at least two rate constants which are determined as rapid and slow endocytosis [5,6], while other authors distinguish between slow, rapid and ultrafast endocytosis [7]. A special fast form of endocytosis retrieves more membrane than the amount that was exocytosed during a proceeding stimulus [5,8]. These different kinetics of endocytosis were unknown before the advent of high time resolved capacitance measurements [9,10]. It was proposed that the slow endocytotic rate is linked to clathrin coated vesicle-dependent membrane recapture, while the fast component is basically clathrin independent and corresponds to the 'kiss-and-run' mechanism [11,12]. A central role in endocytosis was assigned to dynamin, a GTPase that was identified as the gene product of the temperature-sensitive mutant shibire in Drosophila [13]. The role of GTP and phosphorylation/dephosphorylation for the regulation of endocytosis was emphasized by the finding that the GTPase activity of dynamin is controlled by PKC and Camkinase II [14]. In this paper, we demonstrate that activation of G-proteins by GTPγS preferentially inhibits rapid endocytosis, and that this block is released by inhibition of protein kinases.

2. Materials and methods

2.1. Cells and buffers

Bovine chromaffin cells were prepared from adrenal medulla glands, cultured as described [15], and used within 2–10 days after preparation. A standard bath medium (SBM) was used containing in (mM): 150 NaCl, 2 KCl, 2 $MgCl_2$, 2 $CaCl_2$, and 20 HEPES–NaOH, pH 7.2 and a pipette internal solution (PIS) in (mM): 100 CsGlu, 20 NaCl, 3 $MgCl_2$, 2 MgATP, 0.2 EGTA, 0.1 $CaCl_2$, 40 HEPES–NaOH, pH 7.2, +0.1 GTPγS or 0.3 GTP, respectively, as indicated in the experiments, at physiological temperature (34–35 °C). Staurosporine (Calbiochem) was administered at a concentration of 2 μM by preincubation for at least 30 min before the experiment.

2.2. Electrical recordings

Pipette: resistances were in the range of 2–3 MΩ and initial access resistances were 4–5 MΩ in the experiments. Membrane capacitance was measured with a SR830-DSP lock-in amplifier (Stanford Research Systems; Stanford, CA) by superimposing an 800 Hz sinusoid of 40 mV peak-to-peak amplitude onto the holding potential of −70 mV. The phase of lock-in amplifier was set by using the series resistance dithering method [9]. Capacitance was calibrated by adding a capacitor of 200 fF to the capacitance neutralization circuit of a modified EPC-7 (Heka; Lambrecht/Pfalz, Germany) patch-clamp amplifier. The outputs of the lock-in amplifier, imaginary part (capacitance) and real part (conductance) of the cell's complex admittance, along with the membrane current and membrane potential were sampled into a Labmaster DMA TL-1 A/D-converter at 350 Hz. Recording (Labmaster Recorder 2.05) and analyzing (WinPCA 3.87) software was self-programmed (http://www.synosoft.de).

2.3. Experimental protocol

Chromaffin cells on coverslips were washed in SBM, transferred into a recording chamber on a temperature-controlled stage of a Nikon inverted microscope, and sealed to the tip of a patch pipette [16]. Whole-cell access was established by applying repetitive short gentle negative pressure pulses to the seal. Stimulation of exocytosis was triggered by electrical depolarization of the cell membrane. The cells were voltage-clamped at −70 mV and were kept for 4 min in this configuration to allow equilibration of PIS with the cytoplasm before the first depolarization pulse. The depolarization to 0 mV lasted for

* Corresponding author. Fax: +49-9131-853-6381.
E-mail address: andreas.henkel@psych.imed.uni-erlangen.de (A.W. Henkel).

Abbreviations: SBM, standard bath medium; GTPγS, Guanosine 5′-[γ-thio] triphosphate; GDPβS, Guanosine 5′-[β-thio] di-phosphate

0014-5793/$22.00
doi:10.1016/j.febslet.2004.06.069

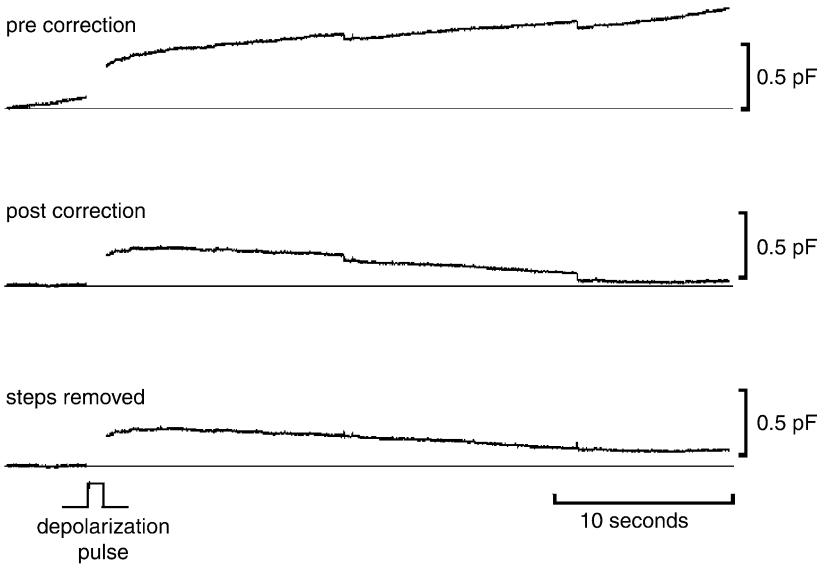

Fig. 1. Correction algorithms for the analysis of endocytosis. All three panels show the same capacitance trace that was recorded from a chromaffin cell in the presence of GTPγS. Before correction, the trace shows a continuous capacitance increase, that represents exocytosis and large steps. At first, this 'steady state' exocytosis was adjusted and then the spontaneous downward steps that represented large endocytotic vesicles were removed.

500 ms and was preceded by a prepulse to −120 mV for 50 ms. Three to four successive pulses were given every 45 s.

2.4. Analysis

The maximum of exocytosis after the end of the pulse was determined by an automated algorithm of the analysis software. In order to distinguish GTPγS-induced exocytosis and step-like events (large vesicles) from depolarization triggered exo-endocytosis, the capacitance trace was processed by an automated computer routine. Fig. 1 illustrates the correction procedure applied to the capacitance trace before the analysis. Pre-depolarization "steady state" exocytosis was subtracted from the capacitance trace in order to quantify exclusively depolarization-induced capacitance changes. In some experiments, large up- or downward steps were detected that resulted from exo- or endocytosis of large vesicles. These events were subtracted from the capacitance trace and analyzed separately.

Student's *t*-test for statistical analysis and determination of time constants by double exponential fits to the capacitance trace was performed by the built-in functions of Origin 6.0 (Microcal).

3. Results

3.1. Multiple distinct mechanisms for endocytosis

Membrane internalization after depolarization-induced stimulation of exocytosis was analyzed in bovine chromaffin cells by whole cell patch clamp capacitance measurements. Pipette solution was equilibrated for 4 min with the cytoplasm before the membrane was depolarized from −70 mV resting potential to 0 mV for 500 ms. Fig. 2A shows a typical experiment where three successive pulses were applied at intervals of 45 s. In the majority of the experiments, the first depolarization pulse triggered the strongest exocytotic response.

Shortly after the pulse, membrane capacitance reached a peak and began to decline steeply, indicating rapid endocytosis. In most experiments, capacitance fell slightly below the starting level. In 6 out of 21 experiments, an ultrafast form of endocytosis was observed after the first pulse (Fig. 2B) and the membrane capacitance decreased far below the original level in these cells. This type of endocytosis was reported earlier with

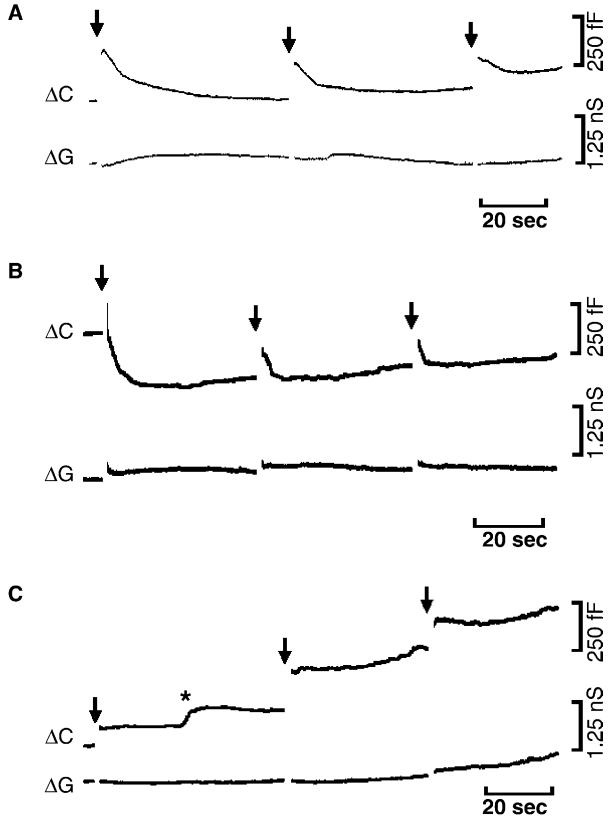

Fig. 2. Exo- and endocytosis in chromaffin cells. Capacitance (Δ*C*) and conductance (Δ*G*) traces, recorded from a chromaffin cell in SBM at 35 °C. Arrows indicate depolarizations for 500 ms from −70 to 0 mV; (A) Three depolarizations trigger exocytosis followed by endocytosis. (B) Same experiment as in (A), but the first depolarization triggered ultrafast excess endocytosis. (C) The cell was dialyzed with 0.3 μM GTPγS. Depolarizations trigger exocytosis but no rapid and no slow endocytosis. Reduced slow endocytosis becomes only apparent after baseline correction. The asterisk (*) indicates a spontaneous burst of exocytosis.

high intracellular calcium concentrations [5,8]. These cells were excluded from the analysis in order to get better comparability.

3.2. Complex effects of GTPγS, dialyzed into chromaffin cells

GTPγS administration triggered spontaneous "steady state" exocytosis and caused inhibition of rapid endocytosis in chromaffin cells. Fig. 2C shows that preferentially the rapid form of endocytosis was strongly inhibited, if the cells were dialyzed with GTPγS. Two additional cellular responses to GTPγS complicated the analysis. First, some cells (6 out of 20) exhibited fast spontaneous bursts of exocytosis as shown in Fig. 3A. These bursts occurred mostly during the first 5 min after break-in and were never seen if GTPγS was administered in combination with staurosporine or GDPβS (data not shown).

Second, GTPγS triggered fusions (exocytosis) and fissions (endocytosis) of large vesicles between 0.8 and 3 μm diameter that contributed considerably to the total membrane traffic. These events were rarely observed before the first depolarization of the cell membrane but increased in frequency during the course of the experiment. Fig. 3B shows three step-like events within 2 s that corresponded to endocytotic vesicles. The average size for endocytotic vesicles was 2.5 μm (±1.24) and 0.977 μm (±0.21) for exocytotic. Detailed analysis showed that endocytosis by large vesicles exceeded exocytosis by 24.5%. However, endocytotic vesicles accounted only for 14.7% of all internalized membranes in GTPγS treated cells. Most of these large vesicles showed transient changes in the corresponding conductance trace that indicated a gradual closing of a fission pore.

3.3. Staurosporine and GDPβS reconstitute rapid endocytosis blocked by GTPγS

Then, we tested if the kinase inhibitor staurosporine or co-dialysis of GDPβS could neutralize the endocytosis block by GTPγS. H7 and calphostin, two more specific PCK-inhibitors, were also tested, but showed no measurable effects (data not shown). Staurosporine decreased depolarization-induced exocytosis by 36.8% but did not change the kinetic characteristics. In order to quantify endocytosis, depolarization-induced capacitance increase was normalized and the resulting traces were averaged. A second order exponential decay fitting to the averaged traces revealed two time constants of rapid and slow endocytosis. Rapid endocytosis in control cells was not significantly (Student's t-test; $P = 0.05$) different from cells treated with GDPβS and staurosporine. The slow endocytotic rate of staurosporine was very similar to the control. GDPβS reduced slow endocytosis by about 50%, compared to control, almost exactly as GTPγS did. Dialysis with GTPγS blocked rapid endocytosis completely and reduced the rate of slow endocytosis significantly. Fig. 4 shows that co-dialysis of GDPβS with GTPγS or co-application of staurosporine revoked the GTPγS induced block of rapid endocytosis completely. The results are quantified and summarized in Table 1. Additionally, slow endocytosis was at least partially reconstituted by staurosporine.

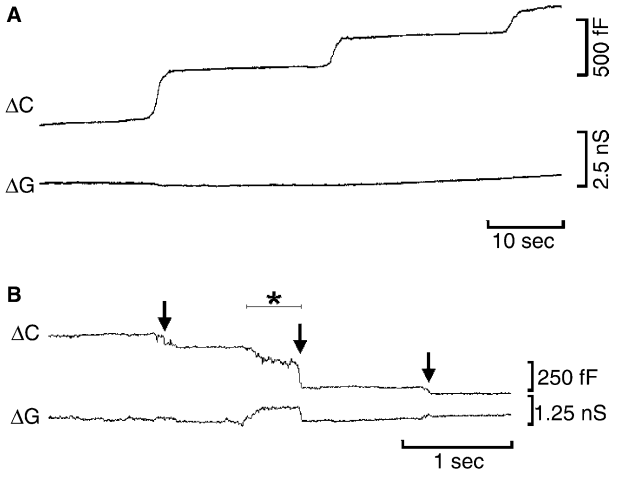

Fig. 3. Effects of GTPγS on exo- and endocytosis. Capacitance (ΔC) and conductance (ΔG) traces, recorded from a chromaffin cell in SBM at 35 °C in the presence of GTPγS; (A) the cell exhibits three spontaneous bursts of exocytosis. (B) Spontaneous downward steps represent endocytosis by large vesicles. The asterisk indicates a fission pore.

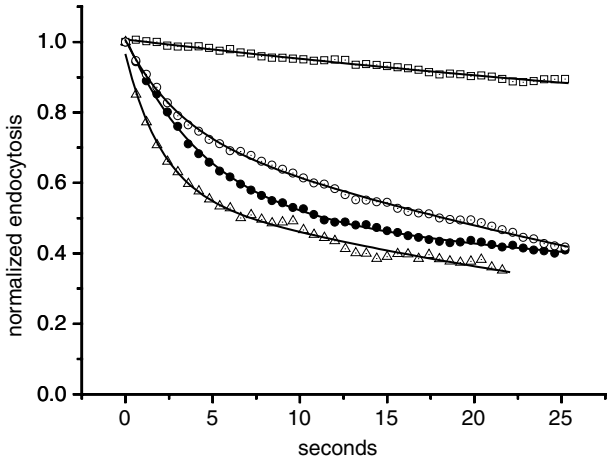

Fig. 4. Inhibition of rapid endocytosis by GTPγS. Averaged and normalized capacitance traces, recorded from chromaffin cells after the end of depolarization pulse. Control cells, $n = 15$, (●); GTPγS + GDPβS, $n = 11$, (○); GTPγS + staurosporine, $n = 9$, (△); GTPγS, $n = 20$, (□).

Table 1
Calculated mean time constants with standard deviations from double exponential fits to endocytotic capacitance traces

Condition	Time constant $\tau 1$	Time constant $\tau 2$
Control	4.3 ± 0.4	29.8 ± 8.5
GTPγS	–	65.6 ± 13.7
GDPβS	4.6 ± 0.7	61.3 ± 21.4
Staurosporine	4.3 ± 0.2	30.4 ± 5.5
GTPγS + staurosporine	2.1 ± 0.5	43.3 ± 10.6
GTPγS + GDPβS	3.0 ± 0.7	60.0 ± 23.4

4. Discussion

We investigated synergistic effects of phosphorylation and G-protein activation on endocytosis in chromaffiin cells. Two different mechanisms of vesicle recycling have been shown in a central synapse model, where the rapid endocytotic component predominates during low to moderate nerve stimulation [17], a

condition that does not trigger an increase of synaptic protein phosphorylation [18]. Tyrosine phosphorylation was suggested to be the main regulatory process of triggering rapid endocytosis [19]. Several proteins essential for endocytosis are subjected to multiple phosphorylation–dephosphorylation cycles [20,21]. These proteins, dynamin I and II, link phosphorylation and GTP-dependent processes. In this study, PKC appears not to be involved in the effects exclusively, because specific inhibitors did not mimic the effect of staurosporine. We found that chromaffin cells use different molecular mechanisms of endocytosis that are characterized by their kinetic parameters and probably by different organelles involved. GTPγS triggers exocytosis via an unknown mechanism and modifies the kinetic of catecholamine release [7,22]. This, of course, complicated the analysis, because we were only able to quantify the combined results of exo- and endocytosis by whole-cell capacitance measurements. In order to separate depolarization-induced exo- and endocytosis from its depolarization-independent, GTPγS triggered form, all traces were processed before analysis as described in the Methods section. However, large endocytotic vesicles in the presence of GTPγS could be identified by whole-cell capacitance and simultaneous conductance measurements. In almost all these cases, fusion- or fission pores were detected. They contributed only 15% to all endocytosed membrane, leaving 85% to small endocytotic vesicles.

It was reported earlier that GTPγS inhibits rapid and slow endocytosis in calf chromaffin cells and arrests the fission of endocytotic vesicles from the plasma membrane [7,23]. We found that GTPγS blocked rapid endocytosis completely; slow endocytosis was reduced, but not abolished, an observation not seen by other authors in similar experiments [7]. This is because our result became only apparent after subtracting GTPγS-induced exocytosis and large vesicles from the capacitance trace, which neutralized these underlying effects.

We further asked whether the block of rapid endocytosis was due to inhibition of GTP hydrolysis or if GTP interfered with the phosphorylation homeostasis.

We were able to show that inhibition of phosphorylation by staurosporine reconstitutes rapid endocytosis after inhibition by GTPγS. This result supports the idea that rapid endocytosis is not dependent on GTP-hydrolysis.

As expected, depolarization-induced exocytosis was largely not affected by the addition of nucleotide analogs, only application of the kinase inhibitor staurosporine reduced stimulated exocytosis slightly (data not shown). This could be explained by staurosporine mediated inhibition of protein kinase C activity which enhances exocytosis [24].

The results of our experiments point to a regulatory role for GTP-binding proteins in rapid endocytosis. The evidence for this conclusion is that non-hydrolyzable GTPγS inhibits rapid endocytosis completely, but parallel application of the kinase inhibitor staurosporine releases the GTPγS-induced block of rapid endocytosis. A potential target molecule could be dynamin I. In general, staurosporine reduces the degree of protein phosphorylation and does not provide any energy for mechanical force. GTPγS reduces, but does not block slow endocytosis, implicating a partially GTP dependent endocytosis pathway. This effect is only observed after subtraction of GTPγS-induced exocytosis (see Section 2). Addition of staurosporine reconstituted slow endocytosis at least partially to the control level. An additional support for the regulatory role of GTP came from co-application of GTPγS and GDPβS. Both nucleotide analogs inhibited slow endocytosis in part, but surprisingly had no additive effects when given together for unknown reasons. Because GDPβS competitively inhibits G-protein activation by GTP and GTP analogs, we propose an active inhibitory role of a yet unknown G-protein in endocytosis.

Taken together, it appears very likely that rapid endocytosis is directly regulated by GTP and dephosphorylation.

Acknowledgements: The authors and this work were supported by the Max-Planck-Gesellschaft.

References

[1] von Grafenstein, H., Roberts, C.S. and Baker, P.F. (1986) J. Cell Biol. 103, 2343–2352.
[2] Burgoyne, R.D. (1995) Pflugers Arch. 430, 213–219.
[3] Galas, M.C., Chasserot-Golaz, S., Dirrig-Grosch, S. and Bader, M.F. (2000) J. Neurochem. 75, 1511–1519.
[4] Sever, S., Damke, H. and Schmid, S.L. (2000) Traffic 1, 385–392.
[5] Smith, C. and Neher, E. (1997) J. Cell Biol. 139, 885–894.
[6] Henkel, A.W. and Almers, W. (1996) Curr. Opin. Neurobiol. 6, 350–357.
[7] Artalejo, C.R., Henley, J.R., McNiven, M.A. and Palfrey, H.C. (1995) Proc. Natl. Acad. Sci. USA 92, 8328–8332.
[8] Engisch, K.L. and Nowycky, M.C. (1998) J. Physiol. 506, 591–608.
[9] Joshi, C. and Fernandez, J.M. (1988) Biophys. J. 53, 885–892.
[10] Nusse, O. and Lindau, M. (1988) J. Cell Biol. 107, 2117–2123.
[11] Artalejo, C.R., Elhamdani, A. and Palfrey, H.C. (1998) Curr. Biol. 8, R62–R65.
[12] Henkel, A.W., Kang, G. and Kornhuber, J. (2001) J. Cell Sci. 114, 4613–4620.
[13] Sontag, M, Fykse, E.M., Y, Liu, J.P., Robinson, P.J. and Südhof, T.C. (1994) J. Biol. Chem. 269, 4547–4554.
[14] Robinson, P.J., Sontag, J.M., Liu, J.P., Fykse, E.M., Slaughter, C., McMahon, H. and Südhof, T.C. (1993) Nature 365, 163–166.
[15] Parsons, T.D., Coorssen, J.R., Horstmann, H. and Almers, W. (1995) Neuron 15, 1085–1096.
[16] Henkel, A.W., Meiri, H., Horstmann, H., Lindau, M. and Almers, W. (2000) EMBO J. 19, 84–93.
[17] Sun, J.Y., Wu, X.S. and Wu, L.G. (2002) Nature 417, 555–559.
[18] Dunkley, P.R., Baker, C.M. and Robinson, P.J. (1986) J. Neurochem. 46, 1692–1703.
[19] Nucifora, P.G. and Fox, A.P. (1999) J. Neurosci. 19, 9739–9746.
[20] Chan, S.A. and Smith, C. (2001) J. Physiol. 537, 871–885.
[21] Cousin, M.A. and Robinson, P.J. (2000) J. Neurochem. 75, 1645–1653.
[22] Graham, M.E., O'Callaghan, D.W., McMahon, H.T. and Burgoyne, R.D. (2002) Proc. Natl. Acad. Sci. USA 99, 7124–7129.
[23] Takei, K., McPherson, P.S., Schmid, S.L. and DeCamilli, P. (1995) Nature 374, 186–190.
[24] Terbush, D.R. and Holz, R.W. (1990) J. Biol. Chem. 265, 21179–21184.